

RSC Advances



This is an *Accepted Manuscript*, which has been through the Royal Society of Chemistry peer review process and has been accepted for publication.

Accepted Manuscripts are published online shortly after acceptance, before technical editing, formatting and proof reading. Using this free service, authors can make their results available to the community, in citable form, before we publish the edited article. This *Accepted Manuscript* will be replaced by the edited, formatted and paginated article as soon as this is available.

You can find more information about *Accepted Manuscripts* in the [Information for Authors](#).

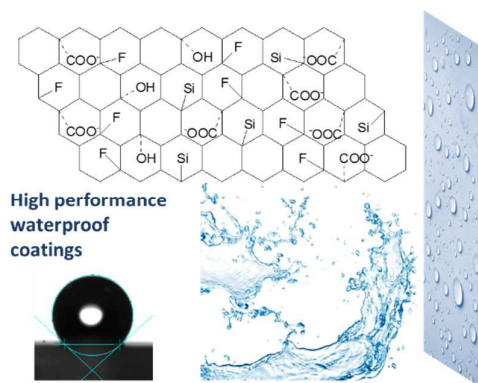
Please note that technical editing may introduce minor changes to the text and/or graphics, which may alter content. The journal's standard [Terms & Conditions](#) and the [Ethical guidelines](#) still apply. In no event shall the Royal Society of Chemistry be held responsible for any errors or omissions in this *Accepted Manuscript* or any consequences arising from the use of any information it contains.

Graphical Abstract

Structural engineering of waterborne polyurethane for high performance waterproof coatingsFangfang Yu,^a Xiangyu Xu,^a Naibo Lin*^a and Xiang Yang Liu*^{b, a}^a Research Institute for Biomimetics and Soft Matter, Xiamen University, Xiamen, 361005, China.^b Department of Physics, National University of Singapore, 2 Science Drive 3, Singapore, 117542, Singapore.

* Corresponding author: Tel.: +65-6516 2812; Fax: Fax: +65-6777 6126

E-mail address: linnaibo@xmu.edu.cn (N. B. Lin); phyluxy@nus.edu.sg (X. Y. Liu)



Novel waterborne polyurethane containing fluorine and siloxane (FSPU) for excellent thermal performance, waterproof and mechanical properties.

Structural engineering of waterborne polyurethane for high performance waterproof coatings

Cite this: DOI: 10.1039/x0xx00000x

Fangfang Yu,^a Xiangyu Xu,^a Naibo Lin^{*a} and Xiang Yang Liu^{*b, a}

Received 00th January 2012,
Accepted 00th January 2012

DOI: 10.1039/x0xx00000x

www.rsc.org/

A series of modified waterborne polyurethanes were synthesized using a self-emulsifying method for high performance waterproof coatings, such as fluoride polyurethane (FPU), siloxane modified waterborne polyurethane (SPU) and the polyurethane containing fluorine and siloxane (FSPU). The structures of waterborne polyurethane were designed from scratch, and the contents of fluoride acrylic monomer (FMA) and siloxane contents (HO-PDMS) segments in FSPU were adjusted for high performance waterproof. It's found that the sample has lowest water absorption, higher water contact angles, and better mechanical/thermal properties, when the FMA content is 20wt% and HO-PDMS content is 3wt%. The mechanisms of improvement of contact angles were investigated, due to the vinyl group crosslinking, higher temperature can significantly improve the hydrophobicity of the films in emulsion polymerization and film forming process. Optimized FSPU has a promising future as a kind of waterborne waterproof coatings.

1. Introduction

Polyurethane (PU) is a series of synthetic copolymers that contain the duplicate carbamate groups in their molecular chain¹, which can be applied in plastics, elastomers, coatings², adhesives, synthetic leather and fibres etc., due to the excellent processing performance³. Polyurethane coating, prepared in organic solvents, has many outstanding properties⁴, such as film forming ability, flexibility, adhesion, abrasion resistance, low temperature resistance, solvent resistance and biological aging resistance. However, considering the increasing solvent price, healthy and environmental problems (e.g., toxicity), organic solvents should be replaced⁵. Waterborne polyurethane (WPU) using water as solvent or dispersant is quite eco-friendly⁶, which not only mainly remains original properties, but also adds the distinctive properties like low viscosity at high molecular weights, non-toxicity, non-polluting, low cost, good applicability and safety.

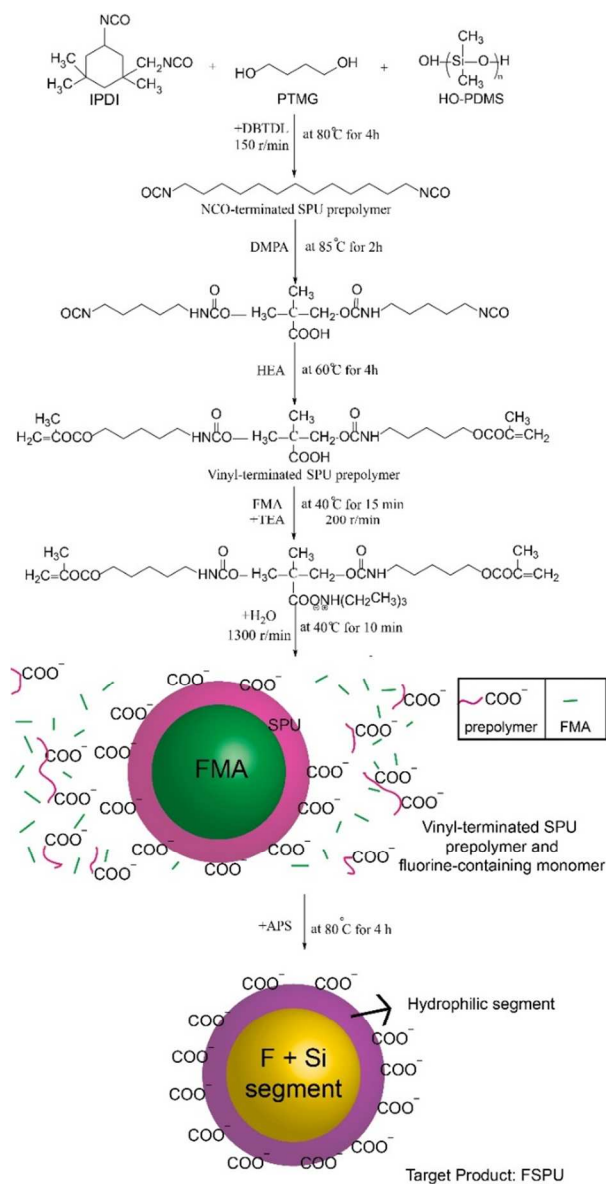
Recently, WPU is reported for waterproof coating⁷. There are two elements, which can be introduced into polyurethane for the improvement of water resistance, one is fluorine, and the other is siloxane. Owing to the polarity and electronegativity, fluorine atom modified polymer obtains high waterproof performance⁸. Fluorinated polyurethane-acrylate (FPU) has many practical and desirable features such as good adhesion, high resistance (to water, oil) and excellent weather ability⁹. Polyurethane with an acrylic polymer containing fluorine component

was reported¹⁰, with increasing the content of fluoride acrylate from 0% to 40%, the hydrophobicity and crosslinking degree of waterborne polyurethane were improved. However, the poor thermal stability and the high price of fluorinated polyurethane lead to a limitation of large-scale use. In addition, heavy fluorinated PU lead to long curing time. As we known, organic silicon also has low surface energy, which has been widely used to produce waterproof coatings. Siloxane-modified polyurethane (SPU) has high thermal resistance properties with low cost compared to fluorinated polyurethane, while possesses poor oil resistance and adhesion.¹¹

In this study, we used the siloxane instead of part of fluoride monomers, which not only can reduce the cost of products, but also can harmonize the properties of FPU and SPU. As we known, the siloxane has a better compatibility compared with fluorinated monomers in polyurethane chains¹², herein, the improvement of the compatibility and performance is the key issue in our system. It becomes very critical to design the modified polyurethane structure and tune the ratio of fluorinated and siloxane-modified segments to pursue better water contact angles (hydrophobic and oleophobic properties), surface energies, mechanical and thermal properties. Importantly, the mechanism of hydrophobicity enhancement was investigated based on the processes of polymerization and film forming. The resulted fluorinated silicone-modified polyurethane (FSPU) shows a promising application in waterproof coating.^{2b, 13}

2. Experimental Section

2.1 Materials



Scheme 1 The preparation process of FSPU emulsions

Poly (tetramethylene oxide glycol) (PTMG, number-average molecular weight = 2000 g/mol, Aladdin Reagents, Shanghai, China), polydimethylsiloxane (HO-PDMS, 700CS, Rongli Chemical Co., Ltd. China) were dried at 110°C under vacuum for 12 hours before use. Dimethylol propionic acid (DMPA, Aladdin Reagents, Shanghai, China) was dried in a vacuum oven at 110°C for 5 h. Isophorone diisocyanate (IPDI, Aladdin Reagents, Shanghai, China), 1,4-butanediol (BDO, Xilong Chemical Co., Ltd. Zhejiang, China) and triethylamine (TEA, Xilong Chemical Co., Ltd.) were used after dehydration with 4A molecular sieves for 1 day. Dibutyltin dilaurate (DBTDL, Aladdin Reagents, Shanghai, China), 2-hydroxyethyl acrylate (HEA, Aladdin Reagents, Shanghai, China), Dodecafluoroheptyl methacrylate (FMA, Silworld Chemical

Co., Ltd. Wuhan, China) and ammonium persulfate (APS, Aladdin Reagents, Shanghai, China) were used as received.

2.2 Synthesis of WPU, FPU, SPU and FSPU

The emulsion of FSPU was prepared according to the procedure shown in Scheme 1. IPDI, PTMG, HO-PDMS and moderate DBTDL were first added into a 250 ml four-necked flask with a reflux condenser, a mechanical stirrer, and an inlet for dry nitrogen. The prepolymerization of polyurethane was carried out at 80°C under N₂ atmosphere for 4 h until the NCO content reached the theoretical value (NCO-terminated prepolymer). A suitable amount of acetone to decrease the viscosity of pre-polymer, the self-emulsifier DMPA was added into the system for 2 h. Then the chain extenders HEA and BDO were added into the system at 60°C for 4 h. After the emulsion was cooled down to room temperature, the neutralization agent TEA and FMA (the mass ratio of FMA is 20 wt%) were added into this flask, the TEA reacted with the carboxylic group in the side chain of vinyl-terminated prepolymer. After 15 min neutralization, distilled water was added to the flask with vigorous stirring to obtain a SPU/FMA hybrid emulsion with a solid content of about 30%. At last, ammonium persulfate (APS, 3wt% of acrylic monomers) was added to the emulsion, and radical emulsion polymerization of acrylate groups (vinyl group) was performed by heating the mixture to 80°C for about 4 h. The emulsion polymerization mechanism was developed by Smith and Ewart,¹⁴ and Harkins¹⁵. Accordingly, in the oil-in-water emulsion, vinyl-terminated pre-polymer as self-emulsifier has hydrophilic groups COO⁻ on the chains, FMA is the hydrophobic monomer. At the first stage, a monomer was dispersed or emulsified in a solution of surfactant (self-emulsifier) and water forming relatively large droplets of monomer in water. Vinyl-terminated pre-polymer created micelles in the water, small amounts of FMA monomer diffused through the water to the micelle. Water-soluble initiator APS was introduced into the water phase where it reacted with monomer in the micelles. At the second stage, the initiator typically reacted in the micelle and not the monomer droplet, both monomer droplets and polymer particles were present in the system. At last, the free monomer droplets disappeared and all remaining monomer was located in the particles. After removal of acetone from the emulsion by rotary vacuum evaporation, aqueous dispersions FSPU with different siloxane content of 3 wt%, 6 wt%, 8 wt% and 10 wt% were prepared. These samples were named as FSPU3, FSPU6, FSPU8 and FSPU10, respectively.

The preparation of WPU, FPU (FPU3, FPU7, FPU10, FPU15, FPU20 and FPU30) and SPU (SPU3, SPU6, SPU8, SPU10) is similar to FSPU (Scheme S1, S2 and S3). The compositions of WPU, FPU, SPU and FSPU emulsions are shown in Table 1.

2.3 Preparation of hybrid films

The hybrid films were prepared by pouring a certain amount of the dispersions onto a Teflon mould or slide glass. The films dried under ambient conditions for 12 h and then dried in an oven for 24 h.

Table 1 The compositions of WPU/FPU/ SPU/ FSPU

Sample	Composition of PU								
	IPDI (molar)	PTMG (molar)	HEA (molar)	DMPA (molar)	BDO (molar)	TEA (molar)	Water (g)	PDMS (wt%)	FMA (wt%)
WPU	0.015	0.005	0.004	0.0055	0.0025	0.0055	36	0	0
FPU3	0.015	0.005	0.004	0.0055	0.0025	0.0055	37	0	3
FPU7	0.015	0.005	0.004	0.0055	0.0025	0.0055	39	0	7
FPU10	0.015	0.005	0.004	0.0055	0.0025	0.0055	40	0	10
FPU15	0.015	0.005	0.004	0.0055	0.0025	0.0055	43	0	15
FPU20	0.015	0.005	0.004	0.0055	0.0025	0.0055	45	0	20
FPU30	0.015	0.005	0.004	0.0055	0.0025	0.0055	52	0	30
SPU3	0.015	0.005	0.004	0.0057	0.0021	0.0057	37	3	0
SPU6	0.015	0.005	0.004	0.0059	0.0017	0.0059	38	6	0
SPU8	0.015	0.005	0.004	0.006	0.0014	0.006	39	8	0
SPU10	0.015	0.005	0.004	0.0061	0.0012	0.0061	40	10	0
FSPU3	0.015	0.005	0.004	0.0057	0.0021	0.0057	46	3	20
FSPU6	0.015	0.005	0.004	0.0059	0.0017	0.0059	48	6	20
FSPU8	0.015	0.005	0.004	0.006	0.0014	0.006	49	8	20
FSPU10	0.015	0.005	0.004	0.0061	0.0012	0.0061	50	10	20

2.4 Characterization

Fourier transform infrared (FTIR) of the FPU/SPU/FSPU thin films were measured using the attenuated total reflectance model (Nicolet IN10, Thermo Fisher Scientific Co., USA) in the range from 4000 to 400 cm^{-1} . Surface analysis was carried by XPS (PHI Quantum 2000 Scanning ESCA Microprobe, Physical Electronics, USA) using a monochromatic $\text{AlK}\alpha_{1,2}$ X-ray source (15 kV, 35 W) and a spot size 200 $\mu\text{m}\times 200 \mu\text{m}$. The samples for XPS were prepared by casting the polymer onto a clean glass disc. Dynamic light scattering (DLS) measurements were carried out to determine the diameter of the particles using a Malvern Mastersizer 2000 (UK). The morphology of emulsion particles were characterized on a transmission electron microscope (TEM, JEM-2100, Japan) using 2% aqueous phosphotungstic acid as a staining agent. The morphology of the films was observed under a SU70 (Hitachi, Japan) scanning electron microscopy (SEM).

The film samples for contact angle measurement were prepared by pouring 120 μL aqueous dispersions on a hydrophilic glass (25mm \times 38mm) surface and dried under ambient conditions for 12 h, then dried at 80 $^{\circ}\text{C}$ or 110 $^{\circ}\text{C}$ for 24

h under atmospheric pressure. The contact angles of water and ethylene glycol droplets on the cured film were measured with a contact angle goniometer (DSA100, Dataphysics Co., Germany) using the sessile-drop method at 25 $^{\circ}\text{C}$ and the reported results are the mean of ten measurements. The contact angle, which is a measure of the surface wettability, was used to assess the hydrophobicity and hydrophilicity. The surface energy of the dried film can be calculated using the following equation:

$$\gamma_s = \gamma_s^d + \gamma_s^p \quad (1)$$

$$\gamma_L(1 + \cos\theta_L) = 2(\gamma_L^d\gamma_s^d)^{1/2} + 2(\gamma_L^p\gamma_s^p)^{1/2} \quad (2)$$

where γ_s is the surface energy of solid film, γ_s^d is the dispersion force, and γ_s^p is the polarity force. The testing liquids used were water (L1) and ethylene glycol (L2), and their γ_{L1}^d , γ_{L1}^p , γ_{L2}^d and γ_{L2}^p were known values that can be obtained from the relevant criteria.

The water resistance (WR) and oil resistance (OR) properties of the solid film were characterized by the solvent absorptions in water and n-heptane, respectively. The weighed cured film was dipped in deionized water or n-heptane at room

temperature for 72 h. The swelling of the films was calculated by using the following equation:

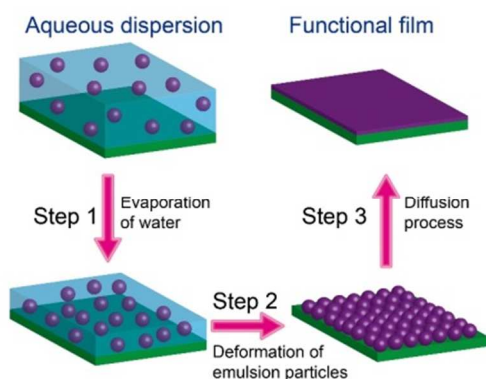
$$\text{Swelling (\%)} = 100 \times (W - W_0) / W_0 \quad (3)$$

where W_0 and W represent the film weights before and after absorbed water/n-heptane, respectively.

The UV-vis transmittance spectrum was measured using a Lambda 750 spectrophotometer (PerkinElmer Co., USA) in the range from 800 to 250 nm. The viscosity of the emulsions was measured at 25°C using Rheo-Microscope MCR302 (Anton Paar Co., Austria). The tensile properties were measured at room temperature using a Universal Testing Machine (UTM, Shimadzu Co., Japan). A cross-head speed of 500 mm/min with gauge length of 2 mm was used to determine the ultimate tensile strength and modulus as well as the elongation at break. The samples for tensile test were prepared by pouring 2mL emulsions into a Teflon mould (150mm×10mm×2mm) and curing at room temperature for 24 h, finally dried at 80°C for 12 h. Thermal gravimetric analysis (TGA) of solid films was carried out using a STA 449F3 (Netzsch Co., Germany) thermal gravimetric analyzer in the range from room temperature to 600°C at a heating rate of 10°C/min under nitrogen atmosphere.

3. Results and discussion

3.1 Film forming process of FSPU



Scheme 2 Film forming process of the hybrid film with hydrophobic surface

The illustration of the forming process of the hybrid films is shown in Scheme 2. The process can mainly be divided into three stages. (1) The first stage is the evaporation of water, the emulsion particles are close to each other to achieve near-packed state with the evaporation of water in waterborne PU. (2) The second stage is the deformation of emulsion particles, when the water evaporated a lot, emulsion particles begin to contact. As the water continue to decline, the protective layer of aqueous polyurethane emulsion particles is damaged. The gap between emulsion particles becomes more and more narrow, the particles tightly pack together until the gap becomes into a capillary. Capillarity forces emulsion particles begin to deformation, emulsion particles gradually changed from spherical to hexahedron until the interface between particles disappeared. (3) The third stage is the diffusion process: the coil shaped polymers in

emulsion particles are close to each other, the chain end mutual diffusion and chain structure mutual fusion, eventually the demulsification and phase inversion partially occurs, phase inversion partially occurs, especially at the interface of the emulsion and air. Because the solubility of WPU, PDMS and FMA in water is different, hydrophobic PDMS and FMA will migrate and enrich at the surface of the film and air with low surface energy, while some hydrophilic groups like COO⁻ and -NH- will migrate and enrich at the interface of film and substrate. Thus, a continuous film with hydrophobicity is formed due to the migration of the atoms with low energy^{30, 47}.

3.2 FTIR spectra and surface compositions of the sample films

Figure 1 shows Fourier Transform Infrared Spectroscopy (FTIR) spectra of IPDI, FMA, WPU, FPU30, SPU10 and FSPU8 films. From the FTIRs of IPDI and FMA, it can be seen that the characteristic bands of NCO and C=C at 2270 cm⁻¹ and 1713 cm⁻¹ respectively, these two peaks disappeared in spectres of WPU, FPU30, SPU10 and FSPU8, this result indicated the complete reaction of raw material. Compared to WPU, the spectra of FPU and FSPU display the CF₂ absorption at 1160 cm⁻¹, meanwhile, SPU10 show the absorption of CH₃ connecting Si at 1259 cm⁻¹, Si-O at 1026 cm⁻¹ and rocking CH₃ connecting Si at 805 cm⁻¹. In addition, a distinct peak at 961 cm⁻¹ presenting the peak of C-H of CH₂CF₃ also appeared in the spectra of FPU and FSPU. This result implied that silicon and fluorine had been successfully introduced into the polyurethane chain.⁹

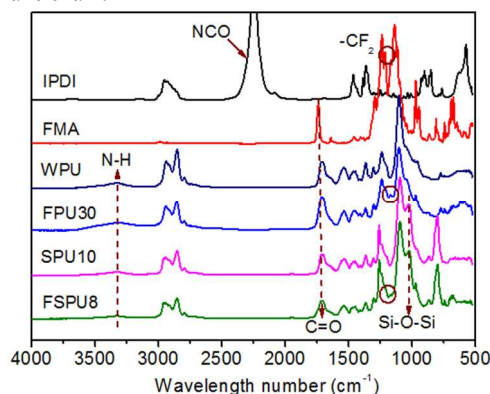


Figure 1 FTIR spectra of IPDI, FMA, WPU, FPU30, SPU10 and FSPU8

X-ray photoelectric spectroscopy (XPS) is a surface chemical analysis technique for analysing the surface chemistry of a material. Figure 2 presents the XPS spectra of WPU, FPU20, SPU10 and FSPU10. The peaks of F1s and Si2p were not observed in WPU. While in the spectrum of FSPU6, the peak of Si2p at 100eV and the peak of F1s at 690 eV were both found. From this result we can know the siloxane and fluorine were introduced into this system successfully. The results of XPS were consistent with that of FTIR result. In addition, the peak intensity of N1s was weak due to the very small amount of hydrophilic urethane groups in the surface layer.

It is well known that the low surface energy of the component provides a thermodynamic driving force for migration to the

polymer-air interface¹⁶. Table 2 displays the fluorine and silicon atomic percentage of the WPU hybrids containing FMA or HO-PDMS. From the Table 2, the fluorine and silicon concentrations of the polymer-air surfaces for all samples are much higher than concentrations of polymer-substrate interfaces. In addition, the oxygen concentrations of surfaces are lower than interfaces, which imply that the surface is enriched with fluorine and silicon segments. The fluorine atomic percentages in the surfaces of FPU10 (content of FMA in polymer: 10 wt %) increase up to about 5.3 %, while in interfaces is just 0.6. The silicon in the surface and interface of SPU10 (content of HO-PDMS in polymer: 10 wt %) are 24.1% and 22.6%, respectively. For FSPU10, the surfaces and interfaces of the silicon percentages are 23.1% and 21.7%, the fluorine percentages are 2.5 and 0.6 respectively. These results show that the fluorinated component and siloxane were enrichment on the surfaces of hybrid films as expected.

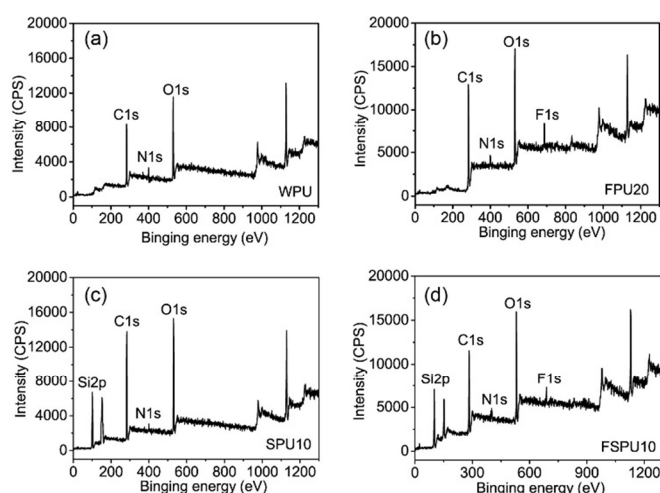


Figure 2 XPS spectra of (a) WPU, (b) FPU20, (c) SPU10 and (d) FSPU10.

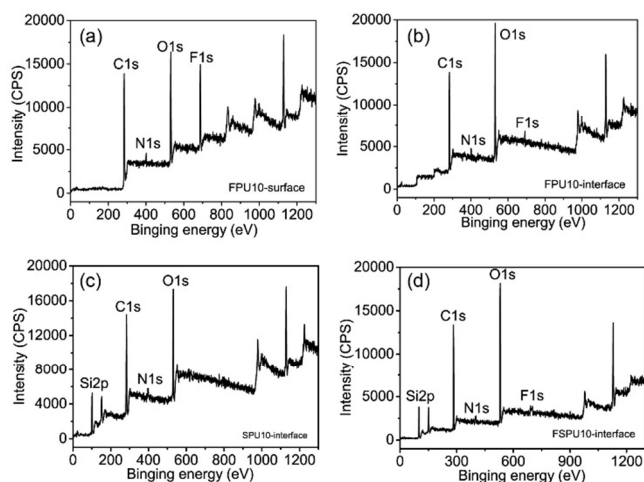


Figure 3 XPS spectra of (a) surface of FPU10, (b) interface of FPU10, (c) interface of SPU10 and (d) interface of FSPU10.

Table 2 Atomic concentration of the surface/interface on hybrid films

Sample	Surface/interface	Atomic concentration (%)				
		C1s	O1s	N1s	F1s	Si2p
FPU10	surface	62.1	32.2	0.4	5.3	0
	interface	62.9	35.9	0.6	0.6	0
SPU10	surface	51.1	24.6	0.2	0	24.1
	interface	50.2	26.8	0.4	0	22.6
FSPU10	surface	49.9	24.3	0.2	2.5	23.1
	interface	50.7	26.6	0.4	0.6	21.7

3.3 The morphology and sizes of emulsion particles

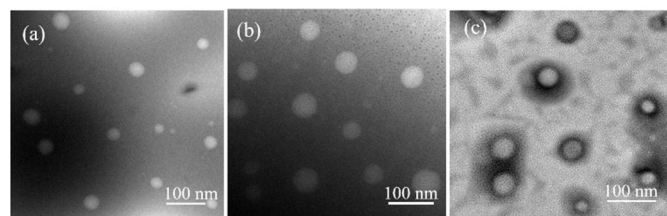


Figure 4 TEM photographs of (a) WPU, (b) FPU10 and (c) FSPU6. Staining acid: 2% aqueous phosphotungstic acid.

Figure 4 shows the TEM images of WPU, FPU10 and FSPU6. These three TEM photographs indicated the PU particles were spherical. The particle sizes of the samples were tested by DLS. From the Table 3, the average particle size of WPU dispersion was about 73.67 nm, when the content of fluorine increased to 30 wt%, the particle sizes of FPU30 reached 290.6 nm (Fig. S1). When the content of siloxane increased to 10 wt%, the particle sizes of SPU10 increased to 145 nm (Fig. S2). FSPU6 shows the similar trend (Figure 5). With increasing the hydrophobic segments of fluorine and siloxane, the hydrophilic segments correspondingly decreased. Based on the emulsion polymerization theory, the diameters of latex particles trend to raise to keep the emulsion stable¹⁴.

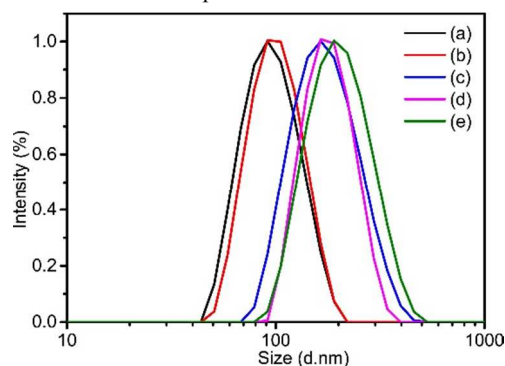


Figure 5 Particle sizes and distributions of (a) FPU20, (b) FSPU3, (c) FSPU6, (d) FSPU8 and (e) FSPU10 dispersions.

From the table 3 we can know the obtained emulsions of FSPU containing 0-8 wt% HO-PDMS content were stable after 3 months, while the FSPU10 was unstable, suggesting that approximately 10

wt% of the siloxane monomer was beyond the self-emulsifying ability of the hybrid emulsion using a fixed content of neutralized DMPA, as a self-emulsifier.

Table 3 Viscosity, average particle size, contact angle and storage stability of FSPU hybrid emulsions

Sample	Viscosity (Pa·s) ^a	Average particle size	Contact angle ^b	Film stability	Storage stability ^c
FSPU3	0.31	145	126.44	yellowish	Stable
FSPU6	0.19	168	128.82	colorless	Stable
FSPU8	0.11	177	107.63	colorless	Stable
FSPU10	0.07	194.8	105.37	colorless	Unstable

^a The viscosity of $\gamma = 10$; ^b The film was dried at 110 °C; ^c The storage stability after 3 months.

3.4 The viscosity of the hybrid polyurethane emulsions

The viscosity of the FSPU emulsions is evaluated by Rheo-Microscope measurement. As shown in table 3, the viscosity of the hybrid emulsion decreased with increasing siloxane monomer content at the shear rate 10. At that shear rate, the interaction force among the polymer chains play a critical role on the viscosity¹⁰. The siloxane segment has a litter polarity and small intermolecular force. The introduction of siloxane on PU will reduce the interaction force and hydrogen bonding between different chains and molecules. So the viscosity decreased with the increase of HO-PDMS.

3.5 Surface morphology of different films

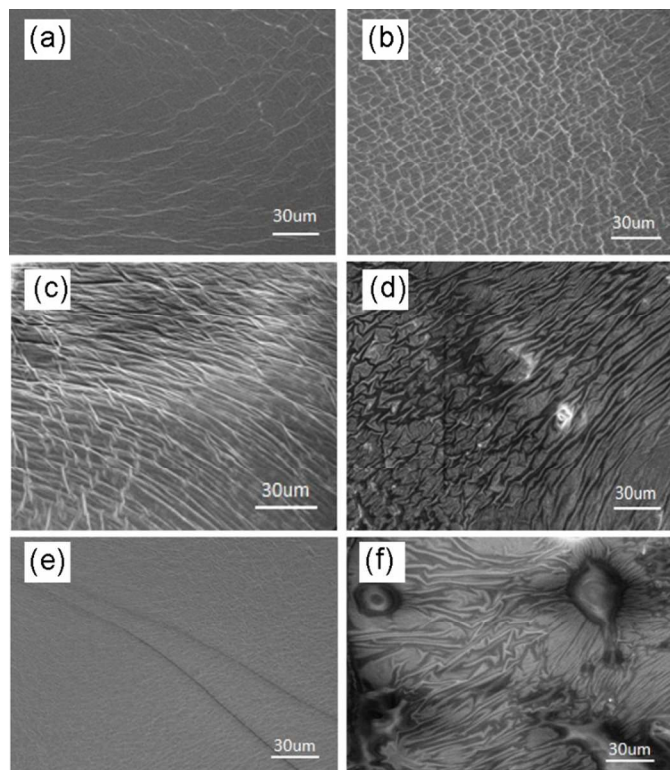


Figure 6 SEM images of different sample films (a) FPU15 (b) FPU20 (c) SPU6 (d) SPU8 (e) FSPU6 (f) FSPU8.

As we known, the solubility parameters of silicone and polyurethane is very different (7.2 and 10.0 respectively), the introduction of siloxane can generate phase separation. There is no any special structure on the WPU film surface, the structure is very homogeneous. Figure 6 shows the surface morphology of different hybrid films. In the figure 6(a-d), the rough surfaces of FPU and SPU consisted of sub-micro papillae and micro wrinkles were formed due to the phase separation. With the increase of fluorine and siloxane content, the phase separations became serious. In the figure 6e, when the fluorine content is at 20 wt%, the addition of a little of siloxane can maintain the compatibility between the fluorine monomers and PU resin. That hints the siloxane has a better compatibility compared with fluorinated monomers in polyurethane chains¹², which improves the compatibility between hydrophilic and hydrophobic segments. However, when the content of siloxane was higher than 6 wt%, the phase separation became so severe that a homogeneous structure was completely destroyed (c.f. Figure 6f).

3.6 The surface properties of polyurethane films

In this experiment, a series of FSPU film samples with different film-forming temperatures were prepared. Figure 7(a) and (b) show the contact angles and surface energies (SE) of film samples dried at 80°C and 110°C, respectively. From this figure we can see the contact angles of films dried at 110°C is higher than those dried at 80°C. The contact angles increased firstly and then decreased with increasing siloxane (HO-PDMS) content, while the change of SE is opposite. In addition, the higher temperature did not make the films oxidation, due to the introduction of siloxane.

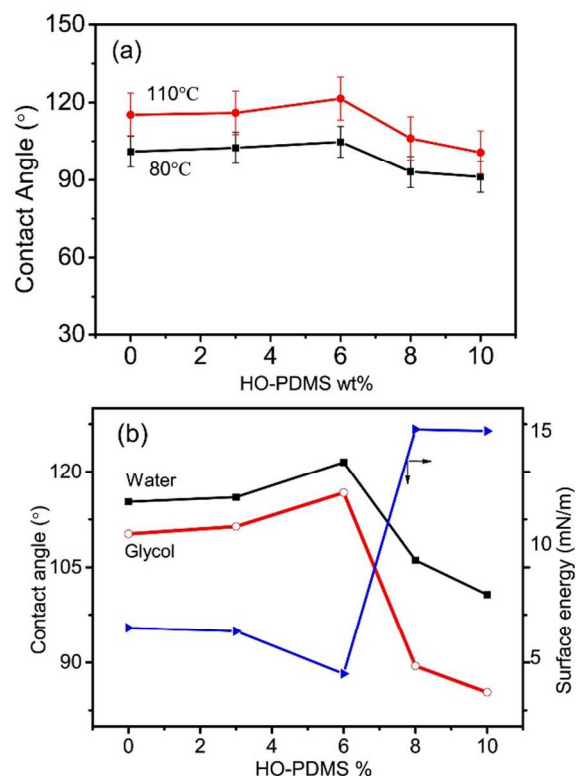


Figure 7 (a) Water contact angles of FSPU hybrid films (b) Surface energy of FSPU hybrid films

Figure S3 and S4 show the results of FPU sample films. We can see the contact angles increased markedly with increasing fluorinated acrylate content to 10 wt%. Further increasing the content of fluorinated monomers (FMA), the contact angles decreased. Figure S5 and S6 show the results of SPU samples, when the siloxane content increased from 0 to 3 wt%, the water and glycol contact angles of the hybrid film samples increased from 110.45° to 117.5°, and from 72° to 110°, respectively. At the same time, the surface energy decreased significantly from 25.09 to 5.31. Compared figure S4 to S6, when the fluorine content is higher than 15%, the contact angles decrease, at the same time, when the siloxane content is higher than 3%, the contact angles also decrease. However, from the results of FSPU, the addition of 3 wt% siloxane does not make the angles decrease, which manifests that the siloxane played a bridging role between fluorine segment and resins. In other words, the siloxane is a certain extent that reduced the phase separation, which is consist with the results of SEM.

3.7 The solvent absorptions of polyurethane films

Water and oil resistances of FSPU films were investigated by the solvent absorptions in water and n-heptane, respectively. From Table 4, FSPU had a low water and oil solvent absorptions due to the common effect of hydrophobic siloxane chains and amphiphobic fluorinated chains. Compared to FPU20, the addition of siloxane can improve the solvent resistance, such as FSPU3 and FSPU6, which further proves that a small amount of siloxane can improve the compatibility of organic fluorine and polyurethane. With increasing the content of HO-PDMS from 3wt% to 10 wt%, the water absorption increased from 38.9% to 142.5%, and the n-heptane absorption increased from 13.9 to 123.2%. The degradation of WR and OR properties is owing to the phase separations. FPU and SPU show the same trend (table S1-2). The low solvent absorptions of FSPU3 polyurethane films had laid a solid foundation for the post-processing in waterproof coatings application, such as the addition of crosslinking agent.

Table 4 UTM results and solvent absorptions of FPU20 and FSPU hybrid films

Sample	Mechanical properties			Solvent absorption	
	Modulus (MPa)	Tensile strength (MPa)	Elongation at break (%)	Water (%)	N-heptane (%)
FPU20	0.2	1.12	468.6	43.9	20.2
FSPU3	0.17	1.03	513.7	38.9	13.9
FSPU6	0.15	0.93	558.7	43.9	14.1
FSPU8	0.11	0.87	575	50.2	65.5
FSPU10	0.08	0.6	610.8	142.5	123.2

3.8 Optical transmittance and mechanical properties of different polyurethane films

The transmittance of films were investigated by UV-vis transmittance spectrometer. A gradual decrease in transmittance of FPU and SPU was observed as the contents of fluorine/siloxane increase, which indicated that the FMA and PDMS contents had an obvious effect on the optical transmittance (fig.S7 and S8). Figure 8 (a) is the UV-vis spectrum of FSPUs. With increasing content of HO-PDMS in FSPUs, a gradual decrease in transmittance was observed in the range of 300-800 nm. The reason is the light scattering caused by a phase separation. The transmittance of our films show better than the one of transparent and hydrophobic waterborne polyurethane coatings containing polydimethylsiloxane reported by Wu et al¹⁷.

Figure 8 (b) is the stress-strain curves of FSPU samples, some specific parameters are shown in Table 4. The tensile strength/modulus of the film samples decreased but the elongation at break increased with increasing siloxane monomer content. The decrease in tensile strength and modulus should be due to the increasing content of soft siloxane segments. On one hand, polyurethane has two phases (soft segment and hard segment). There is a big difference between the solubility parameters of two phases. So the siloxane modified polyurethane is a typical thermodynamic instability system. On the other hand, the steric hindrance of the fluorine atom and the weak polarity of silicon decrease the intermolecular force. Thereby, hybrid samples with higher elongation at break containing higher contents of fluorine monomer and siloxane. The pristine WPU hybrid materials prepared in this study had relatively high tensile strength (Table S1). The tensile strengths of FSPU films decreased greatly from 1.12 MPa to 0.6 MPa, and the modulus dropped from 0.2 to 0.08 MPa and the elongation at break improved from 468.6% to 610.8%.

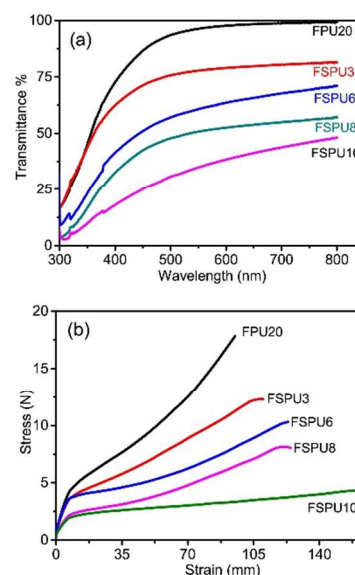


Figure 8 (a) UV-vis results and (b) stress-strain curves of FPU20, FSPU3, FSPU6, FSPU8 and FSPU10

3.9 Thermal stability of polyurethane hybrid films

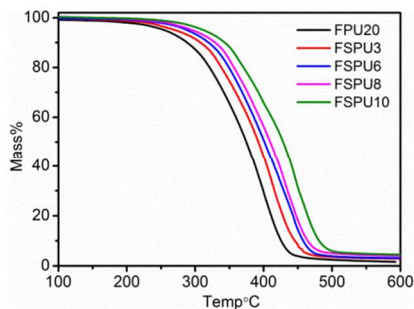


Figure 9 TGA curves of FPU20 and FSPUs.

The thermogravimetric (TG) curves of FSPU films are shown in Figure 9. From this result, all FSPUs have a similar thermal decomposition process. The thermal decomposition temperature of polysiloxane is at around 500 °C¹⁸, and the polyurethane begins to thermal decompose when the temperature reached 300 °C. The figure shows the decomposition temperature of samples containing polysiloxane is higher than the polyurethane FPU20 without siloxane segment. The maximum decomposition temperatures of FSPU8 and FSPU10 are 389 °C and 414 °C, it is much higher than FPU20. And the weight loss rate at around 430 °C is consistent with the resin content in the copolymer. The maximum decomposition temperatures of FSPU3 and FSPU6 are 351°C and 370°C, it is obvious lower than that samples containing higher siloxane content. Thus, the use of organic siloxane to modify polyurethane, can significantly improve the thermal stability of the resin.

3.10 Mechanism of the improvement of contact angles

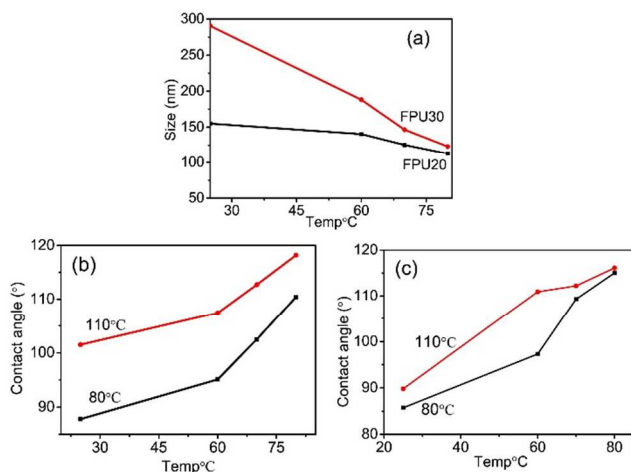


Figure 10 Average particle sizes of (a) FPU20 and FPU30 hybrid films at different polymerization temperature; Water contact angles and polymerization temperature profiles of (b) FPU20 and (c) FPU30 hybrid films, both films were dried at 80 °C and 110 °C.

The mechanisms of the emulsion polymerization and film forming were investigated in our system by tuning the key parameter of temperature. On the step of the polyurethane emulsions, the radical polymerization temperatures of FPU20 and FPU30 were changed from 25 °C to 80 °C. From the DLS results (c.f. Figure 10 (a)), the particle sizes of FPU20 decreased from 155.1 nm to 113 nm, while the FPU30 decreased from 290.6 nm to 123.1 nm, the particle sizes

of FPU20 and FPU30 decreased at the same time as radical temperature rising. Based on the knowledge of emulsion polymerization, in the initial stage, higher radical polymerization temperature can accelerate the initiator decomposition rate, and resulting in the increase of free radicals, the rate of growth rate of molecular chains in a period is lower than the speed of generating new molecular, hinting more nucleation centres formed¹⁹. As the results, the sizes of emulsion particles decreased with rising polymerization temperature. Figure 10 (b) and (c) show the contact angles of FPU20 and FPU30 films at different polymerization temperatures. It can be seen that the hydrophobicity was raised while the polymerization temperature increased. As the hydrophobicity was affected dramatically by the degree of crosslinking in polymer²⁰. It can infer that lower polymerization temperature will generate more residual vinyl groups in the emulsion, and less degree of crosslinking in the films.

On the step of the film forming, FPU20 and FPU30 emulsion polymerized were dried at different temperature. As shown in Figure 10 (b) and (c), the water contact angles of FPU20 and FPU30 films dried at 80 °C and 110 °C. The contact angles increased with film-forming temperatures²¹. Due to the residual vinyl groups, lower film-forming temperature is not helpful for cross-linking reaction, which can weaken the hydrophobicity of films. The films of FSPU, FPU and SPU show similar rule (c.f. Figure S4 and Figure S9).

4. Conclusions

A series of WPU, FPU, SPU, FSPU emulsions were prepared without an external emulsifier. ATR-FTIR, XPS and DLS showed that the target products were prepared and the fluorine/siloxane was grafted to PU chains successfully and the fluorine and silicon on the surfaces of sample films are enrichment. The emulsion displays spherical structure and the particle size was in the range from dozens to several hundred. By measuring solvent absorptions and contact angles of the cured films, within a certain range, it was found that the solvent resistances and hydrophobicity of cured films became better with increasing fluorine and siloxane content compared to the unmodified polyurethane, out of the range the properties is worse gradually. The particle size, elongation at break, thermostability and contact angles of the FSPU samples increased with increasing siloxane content, on the other hand, the viscosity of emulsion, tensile strength, modulus and SE were significantly decreased. As the results, the proper addition of fluorine and siloxane can make the mechanical, thermodynamic and surface properties of hybrid materials maintain at a proper level, which could be controlled easily by adjusting the chemical composition of hybrid materials. In polymerization and film-forming process, the reaction of vinyl groups plays a key role, better hydrophobicity of films was formed under higher temperature. Our study will pave the way to the application of modified waterborne polyurethanes in many waterproof fields, such as corrosion protection of metals and wood. Additionally, the waterborne polyurethane can be functionalized to pursue long-life/ultra-performance functional materials, such as pressure-sensitive polyurethane, fluorescent anti-counterfeiting material, optoelectronic device material and so on.

Supporting Information

The synthesis and characterization of FPU and SPU are described in the supporting information.

Acknowledgments

This work is financially supported by NUS AcRF Tier 1 (R-144-000-348-112), National Nature Science Foundation of China (No. 21404087, U1405226), Fujian Provincial Department of Science & Technology (2014H6022, 2015J05109) and the 1000 Talents Program from Xiamen University.

Notes and references

^a Research Institute for Biomimetics and Soft Matter, Xiamen University, Xiamen, 361005, China.

^b Department of Physics, National University of Singapore, 2 Science Drive 3, Singapore, 117542, Singapore.

* Corresponding author: Tel.: +65-6516 2812; Fax: +65-6777 6126

E-mail address: linnaibo@xmu.edu.cn (N. B. Lin); phyluxy@nus.edu.sg (X. Y. Liu)

- a) B. Ghosh and M. W. Urban, *Science*, 2009, 323, 1458-1460; b) H. Y. Wei, Q. Li, M. Ojelade, S. Madbouly, J. U. Otaigbe and C. E. Hoyle, *Macromolecules*, 2007, 40, 8788-8793; c) A. F. Osman, G. A. Edwards, T. L. Schiller, Y. Andriani, K. S. Jack, I. C. Morrow, P. J. Halley and D. J. Martin, *Macromolecules*, 2012, 45, 198-210; d) S. Chakrabarty, M. Nisenholt and K. J. Wynne, *Macromolecules*, 2012, 45, 7900-7913.
- a) Z. L. Yang, D. A. Wicks, C. E. Hoyle, H. T. Pu, J. J. Yuan, D. C. Wan and Y. S. Liu, *Polymer*, 2009, 50, 1717-1722; b) J. L. Tian, Y. M. Cao and X. T. Zhou, in *Advanced Materials and Structures, Pts 1 and 2*, eds. Y. H. Kim, P. Yarlagadda, X. D. Zhang and Z. J. Ai, Trans Tech Publications Ltd, Stafa-Zurich, 2011, vol. 335-336, pp. 881-885.
- a) J. H. Shi, X. Han and K. L. Yan, *Text. Res. J.*, 2014, 84, 1174-1182; b) S.-F. Zhang, R.-M. Wang, Y.-F. He, P.-F. Song and Z.-M. Wu, *Prog. Org. Coat.*, 2013, 76, 729-735; c) D. Xu, K. Wu, Q. H. Zhang, H. Y. Hu, K. Xi, Q. M. Chen, X. H. Yu, J. N. Chen and X. D. Jia, *Polymer*, 2010, 51, 1926-1933; d) R. Udagama, E. Degrandi-Contraires, C. Creton, C. Graillat, T. F. L. McKenna and E. Bourgeat-Lami, *Macromolecules*, 2011, 44, 2632-2642; e) J. W. Cho, J. W. Kim, Y. C. Jung and N. S. Goo, *Macromol. Rapid Commun.*, 2005, 26, 412-416; f) S. Zhang, M. Guo, Z. Chen, Q. H. Liu and X. Liu, *Colloids Surf. Physicochem. Eng. Aspects*, 2014, 443, 525-534.
- a) K. A. Chaffin, A. J. Buckalew, J. L. Schley, X. Chen, M. Jolly, J. A. Alkatout, J. P. Miller, D. F. Untereker, M. A. Hillmyer and F. S. Bates, *Macromolecules*, 2012, 45, 9110-9120; b) S. H. Hsu, H. J. Tseng and Y. C. Lin, *Biomaterials*, 2010, 31, 6796-6808; c) D. V. Palaskar, A. Boyer, E. Cloutet, C. Alfes and H. Cramail, *Biomacromolecules*, 2010, 11, 1202-1211; d) Z. Dai, Z. H. Li, L. Li and G. W. Xu, *Polym. Adv. Technol.*, 2011, 22, 1905-1911; e) N. B. Lin, X. Y. Liu, Y. Y. Diao, H. Y. Xu, C. Y. Chen, X. H. Ouyang, H. Z. Yang and W. Ji, *Adv. Funct. Mater.*, 2012, 22, 361-368.
- a) A. Dalmais, C. A. Serra, Z. Q. Chang, M. Bouquey and R. Muller, *Macromolecular Materials and Engineering*, 2014, 299, 698-706; b) G. Lligadas, J. C. Ronda, M. Galia and V. Cadiz, *Biomacromolecules*, 2010, 11, 2825-2835; c) Y. S. Lu and R. C. Larock, *Biomacromolecules*, 2007, 8, 3108-3114; d) L. Lei, L. Zhong, X. Lin, Y. Li and Z. Xia, *Chem. Eng. J.*, 2014, 253, 518-525.
- a) T. Zhang, W. J. Wu, X. J. Wang and Y. P. Mu, *Prog. Org. Coat.*, 2010, 68, 201-207; b) K. Kim, M. Kim and J. Kim, *Ceram. Int.*, 2014, 40, 10933-10943.
- a) S. Awad, H. M. Chen, G. D. Chen, X. H. Gu, J. L. Lee, E. E. Abdel-Hady and Y. C. Jean, *Macromolecules*, 2011, 44, 29-38; b) D. H. Park, J. K. Oh, S. B. Kim and W. N. Kim, *Macromolecular Research*, 2013, 21, 1247-1253; c) Y. R. Lee, A. V. Raghu, H. M. Jeong and B. K. Kim, *Macromol. Chem. Phys.*, 2009, 210, 1247-1254; d) X. Y. Gao, Y. C. Zhu, S. Zhou, W. Gao, Z. C. Wang and B. Zhou, *Colloids and Surfaces a-Physicochemical and Engineering Aspects*, 2011, 377, 312-317; e) N. Yousefi, M. M. Gudarzi, Q. B. Zheng, X. Y. Lin, X. Shen, J. J. Jia, F. Sharif and J. K. Kim, *Composites Part a-Applied Science and Manufacturing*, 2013, 49, 42-50.
- B. Kundu, R. Rajkhowa, S. C. Kundu and X. Wang, *Adv. Drug Del. Rev.*, 2013, 65, 457-470.
- S. W. Lee, Y. H. Lee, H. Park and H. Do Kim, *Macromolecular Research*, 2013, 21, 709-718.
- M. Shin, Y. Lee, M. Rahman and H. Kim, *Polymer*, 2013, 54, 4873-4882.
- a) H. Stoyanov, P. Brochu, X. Niu, C. Lai, S. Yun and Q. Pei, *Rsc Advances*, 2013, 3, 2272-2278; b) H. D. Hwang and H. J. Kim, *React. Funct. Polym.*, 2011, 71, 655-665; c) S. W. Zhang, RenLiu, J. Q. Jiang, C. Yang, M. Q. Chen and X. Y. Liu, *Prog. Org. Coat.*, 2011, 70, 1-8; d) A. K. Nanda, D. A. Wicks, S. A. Madbouly and J. U. Otaigbe, *Macromolecules*, 2006, 39, 7037-7043; e) S. A. Madbouly, J. U. Otaigbe, A. K. Nanda and D. A. Wicks, *Macromolecules*, 2007, 40, 4982-4991; f) Y. Xia and R. C. Larock, *Macromol. Rapid Commun.*, 2011, 32, 1331-1337; g) G. N. Li, S. L. Jiang, Y. J. Gao, X. K. Liu and F. Sun, *Ind. Eng. Chem. Res.*, 2013, 52, 2220-2227; h) H. Sardon, L. Irusta, R. H. Aguirresarobe and M. J. Fernández-Berridi, *Prog. Org. Coat.*, 2014, 77, 1436-1442; i) H. Sardon, L. Irusta, M. J. Fernandez-Berridi, M. Lansalot and E. Bourgeat-Lami, *Polymer*, 2010, 51, 5051-5057; j) S. Chakrabarty, X. Zhang, P. Bharti, Y. Chujo, J. Miyake, K. J. Wynne and V. K. Yadavalli, *Polymer*, 2010, 51, 5756-5763; k) T. Ribeiro, C. Baleizao and J. P. S. Farinha, *Materials*, 2014, 7, 3881-3900.
- L. Mammen, X. Deng, M. Untch, D. Vijayshankar, P. Papadopoulos, R. Berger, E. Riccardi, F. Leroy and D. Vollmer, *Langmuir*, 2012, 28, 15005-15014.
- a) A. Lopez, E. Degrandi-Contraires, E. Canetta, C. Creton, J. L. Keddie and J. M. Asua, *Langmuir*, 2011, 27, 3878-3888; b) J. Drelich and E. Chibowski, *Langmuir*, 2010, 26, 18621-18623; c) N. B. Lin, Z. H. Meng, G. W. Toh, Y. Zhen, Y. Y. Diao, H. Y. Xu and X. Y. Liu, *Small*, 2015, 11, 1205-1214.
- I. Penboss, in *Surface Coatings*, Springer, 1993, pp. 294-302.
- W. D. Harkins, *J. Am. Chem. Soc.*, 1947, 69, 1428-1444.
- a) Y. Li, X. J. Huang, S. H. Heo, C. C. Li, Y. K. Choi, W. P. Cai and S. O. Cho, *Langmuir*, 2007, 23, 2169-2174; b) Y.-S. Kim, J.-S. Lee, Q. Ji and J. E. McGrath, *Polymer*, 2002, 43, 7161-7170; c) F. Levine, J. La Scala and W. Kosik, *Prog. Org. Coat.*, 2010, 69, 63-72.
- Z. Wu, H. Wang, X. Tian, P. Cui, X. Ding and X. Ye, *Phys. Chem. Chem. Phys.*, 2014, 16, 6787-6794.
- J.-M. Yeh, C.-T. Yao, C.-F. Hsieh, H.-C. Yang and C.-P. Wu, *Eur. Polym. J.*, 2008, 44, 2777-2783.
- a) P. J. Feeney, D. H. Napper and R. G. Gilbert, *Macromolecules*, 1987, 20, 2922-2930; b) N. B. Lin, Z. Y. Wu, H. Y. Xu and C. Zhang, *Polym. Mater. Sci. Eng.*, 2009, 25, 133-136.
- D. Gan, A. Mueller and K. L. Wooley, *J. Polym. Sci., Part A: Polym. Chem.*, 2003, 41, 3531-3540.
- D. Dieterich, *Prog. Org. Coat.*, 1981, 9, 281-340.